Single and population coding of taste in the gustatory-cortex of awake mice

Abbreviated Title: Taste Processing in Mouse Gustatory Cortex

David Levitan[2] *, Jian-You Lin[1,3] *, Joseph Wachutka[1], Narendra Mukherjee[1], Sacha B. Nelson[2,3,4], Donald B. Katz[1,3]

Departments of Psychology[1] and Biology[2], Volen Center for Complex Systems[3], National Center for Behavioral Genomics[4], Brandeis University, Waltham, Massachusetts 02454, USA.

*These two authors contributed equally to this research.

Proofs and correspondence to corresponding Author:

Donald B Katz, PhD, Brandeis University

Department of Psychology, MS 062, 415 South Street, Waltham, MA 02454,

Email: dbkatz@brandeis.edu

Number of Pages: 31

Figures: 9

Abstract: 249

Introduction: 522

Discussion: 1126

Declaration of Interest: The authors declare no competing financial interests.
Acknowledgements: This research was supported by the National Institute on Deafness and Other Communication Disorders (NIDCD) DC006666.

Abstract

A great deal is known about the broad coding and neural ensemble dynamics characterizing forebrain taste processing in awake rats, and about the relationship between these firing rate dynamics and behavior. With regard to mice, in contrast, data concerning cortical taste coding are few, inconclusive, and largely restricted to imaging—a technique that as of now lacks the temporal sensitivity necessary for evaluation of fast response dynamics. Here we have recorded the spiking activity of ensembles of gustatory cortical (GC) single neurons while presenting representatives of the basic taste modalities (sweet, salty, sour and bitter) to awake mice. Our results reveal deep similarities between rat and mouse taste processing: many recorded murine GC neurons (~66%) responded distinctly to different tastes, and entropy analysis (which measures the breadth of taste coding) confirmed that the majority in fact responded to 3 or 4 tastes; temporal coding analyses further revealed that single mouse GC neurons sequentially code taste identity and palatability—the latter responses emerging ~0.5s after the former—a dynamic that population analysis suggested reflects a reliable sequence of network states activated by taste delivery (i.e., ensembles of simultaneously-recorded neurons transitioned suddenly and coherently from coding taste identity to coding taste palatability). All of the above results held across the anterior-posterior and dorsal-ventral axes of GC—neither between- nor within-mouse mapping revealed regions of narrow or temporally simple taste responses. In conclusion, our data indicates that mouse GC, like rat GC, codes multiple aspects of taste in a coarse, time-varying manner.

Significance

Taste is a useful system with which to study the electrophysiology of cortical coding in relation to behavior. Given the likely contribution of genetics to this subject, it is surprising that there has been almost no work done on the electrophysiology of mouse taste (and that the few imaging studies done on mouse gustatory cortex (GC) have failed to provide consensus on basic features of taste coding). Here we provide the first thorough analysis of taste-related spiking activity in ensembles of awake mouse GC neurons. This analysis reveals deep, abiding similarities between mouse cortical taste processing and that repeatedly demonstrated in rat: mouse GC codes multiple aspects of taste in a coarse, time-varying manner that is essentially invariant across the spatial dimensions of the GC. Mice engage in distributed cortical network processing of taste, rather than coding each specific taste in an all or non-fashion in specific anatomical locations.

Introduction

Mice may be the most commonly used subjects in vertebrate neuroscience research. The use of mice affords researchers relatively easy access to the molecular and genetic underpinnings of network activity, learning-related plasticity, and behavior (Stevens, 1996; Kandel et al., 2014). As taste is a particularly good sensory system with which to study these three topics (see below and Carleton et al., 2010; Maffei et al., 2012), it is surprising that there has been almost no extensive analysis of central taste electrophysiology in awake mice (although see Kusamoto-Yoshida, et al., 2015); *in vivo* murine taste response analyses have almost ubiquitously used imaging data. The results of these analyses have been difficult to reconcile with one another (Chen et al., 2011; Fletcher et al., 2017; Lavi et al., 2018), and with the coherent progress has been made toward characterizing primary gustatory cortical (GC) taste responses in awake rats.

The work on rats has exposed reliable properties of taste spiking activity in relation to behavior, specifically revealing that: 1) responses to multiple tastes appear not only in the same region but also within the same single neurons (Katz et al., 2001; Fontanini & Katz, 2006; Jezzini et al., 2013; Accolla et al., 2007; Samuelsen et al., 2013; Samuelsen & Fontanini, 2017); 2) these responses progress through a series of firing-rate “epochs,” coding in turn the presence, physical properties, and palatability of a taste across 1-1.5s (Katz et al., 2001; Bahar et al., 2004; Sadacca et al., 2012; Maier & Katz, 2013; Samuelsen et al., 2013); 3) late-epoch palatability-related firing is uniquely affected by experience-driven shifts of taste palatability (Bahar et al., 2004; Fontanini & Katz, 2006; Grossman et al., 2008; Moran and Katz., 2014); and 4) in single trials the onset of palatability is a sudden, coherent network phenomenon, the timing of which predicts and impacts behavior (Jones et al., 2007; Sadacca et al., 2016; Li et al., 2016). A test of

whether mouse GC neurons respond in a like manner has not yet been performed; the extant imaging data is incapable of capturing the fast and subtle neural dynamics that characterize rat cortical taste responses.

For the current study, we have recorded the responses of small ensembles of GC neurons (10-39 neurons/ensemble) in awake mice to presentations of stimuli representing four major taste modalities (sweet, salty, sour and bitter). Our data reveal that taste responses in murine GC recapitulate all of the basic principles of taste responses in rat GC: taste delivery evoked broad and dynamic responses that coded first taste identity and then taste palatability; furthermore, these single-neuron dynamics reflected coherent ensemble transitions. We took care to map the spatial extent of GC, and were able to show that each of these response properties are observed uniformly along the anterior-posterior and dorsal-ventral axes; we observed no regions of noticeably sparse responsiveness, and no regions in which responses failed to reflect the general dynamics.

These results offer insight into mouse cortical taste processing—insight that can be used, in conjunction with tools available only in the mouse (among mammals), to delve into the undoubtedly rich relationship between molecular and network analyses of sensory function.

Material and Methods

Subjects

The experimental subjects were C57BL/6J (n = 2) and Stk11tm1.1Sjm (StK11; n = 4) mice. The mice were purchased from Jackson Laboratories (Bar Harbor, ME). Stk11f/f mice have conditional floxed allele between exon 3 and exon 6, which was inactive through the entire set of experiments. These mice were backcrossed after development by the donating investigator for at least 4 generations to C57BL/6J mice and were bred to C57BL/6J for at least one generation upon arrival to Jackson Laboratories (see also Nakada et al., 2010). After the mice were purchased from Jackson Laboratories they were further backcrossed for 3-4 generation to C57BL/6J before establishing a colony. Upon arrival, the mice were placed on a 12-hour light-dark cycle, and given *ad libitum* access to food and water except during experimentation, at which time water access was restricted (see “Fluid delivery protocol”) while food remained available *ad libitum* (note that animals reliably consume less food when thirsty).

No behavioral or neural taste response differences distinguished the strains; they are therefore collapsed into a single group for purposes of our experiments. Experiment procedures started once mice were 60-80 days old. All procedures were approved by the Brandeis University Institutional Animal Care and Use Committee (IACUC) and in accord National Institutes of Health guidelines.

Surgery

Mice were anesthetized with an intraperitoneal (ip) injection of ketamine/xylazine mix (KX; 20mg/ml ketamine, 2.5 mg/ml Xylazine, and 0.5 mg/ml Aceptomazine; total injection volume 5µl/g), and stabilized in a stereotaxic frame. A midline incision on the scalp exposed the skull, and 2 trephine holes were made dorsal to GC. Multi-electrode bundles (16 formvar-coated, 25-µm in diameter nichrome wires) were gradually lowered into the holes, to a spot just above GC: the AP position was ~1.2 mm in front of bregma for anterior GC and ~0.4 mm for posterior GC; the ML positioning was ±3 mm for all mice. Bundles were then lowered to a DV of -2.25 mm from the *pia mater* (prior to recording sessions, bundles were further lowered by 0.25-0.5 mm to reach dorsal GC, and 0.75-1.00 mm to reach ventral GC; see Figure 1 for examples of the identification of the various anatomical locations) and cemented to the skull, along with one intraoral cannula (IOC; flexible plastic tubing inserted into the cheek to allow controlled delivery of tastes to the tongue of awake mice, see below).

In some of the mice, BLA (AP= -1.4, ML= ±3.4, 200 nl injections at DV= 4.3 mm and 4.6 mm from the dura) was infected with AAV2/5::Camk2α-GFP to visualize BLA axons in the ventral GC. This was done to make the separation of dorsal from ventral sub-regions of GC easier to visualize.

Mice were given 7 days to recover from the surgery. During the first 3 days of this recovery, injections of meloxicam (2 mg/kg), ip) and penicillin (0.1 ml), both administered subcutaneously, provided pain and infection management, respectively.

Fluid delivery protocol

For the three days following recovery from surgery, mice received one 30-min session/day in which 60 15-µl aliquots (hereafter, “trials”) of water were delivered. This procedure habituated the mice to the experimental environment, and to IOC delivery of fluid. Following delivery of the last session of water, the electrodes were lowered 250-1000 µm and mice were returned to home cage.

On the day following the third adaptation session, the recording experiment started. The procedure was identical to that described above, except that water was replaced with 4 different taste stimuli, which were sweet (0.2 M sucrose), salty (0.1 M sodium chloride), sour (0.02 M citric acid), and bitter (0.001 M quinine). A total of 15 trials of each taste were delivered, in random order (sampling without replacement). These tastes and concentrations were chosen to provide compatibility to our prior research, and because they provided a broad range of both quality and palatability.

A subset of mice (N=4) received two identical recording sessions separated by one day. In these cases, the electrodes were lowered ~250-500 µm immediately after the first recording session. When data from these two sessions were compared (as a specific part of the study, see below), no substantive between-day differences were noted; the data from the two sessions were therefore otherwise combined.

Acquisition of electrophysiological data

Voltage signals from the micro-electrodes were sampled at 30 kHz, digitally amplified and filtered, and saved to the hard drive of an Ubuntu computer connected to an Intan recording system (RHD2000 Evaluation System and Amplifier Boards; Intan Technologies, LLC, LA). We retained all waveforms from these raw voltage signals, and sorted the waveforms into distinct units using a semi-supervised spike sorting strategy: recorded voltage data were filtered between 300-3000Hz, grouped into potential clusters by a Gaussian Mixture Model (GMM) and refined manually (to enhance conservatism) by the experimenters (for details see Mukherjee et al., 2017). A total of 185 single units were isolated for the experiments across 10 sessions. As has been done many times previously, isolated units were categorized as being either putative pyramidal neurons or putative interneurons on the basis of wave shape and average inter-spike interval (e.g., Bartho et al., 2004; Sirota et al., 2008).

Statistical analysis of neural data

"Taste responsiveness". A single neuron was deemed "taste-responsive" if firing rates changed with taste delivery. Paired t-tests were conducted to determine whether the evoked firing rate (2 seconds post-delivery) significantly differed from its baseline firing rate (2 seconds prior taste delivery). Alpha level was set at $p < 0.05$. This analysis was first performed on firing averaged across taste (providing a general quantification of the neuron's sensitivity to taste input) and then again for each individual taste response. While this results in a relatively large number of statistical comparisons (a common issue for studies of simple coding), the combination of these with the more unified, more conservative analyses described below ensured valid recognition of the nature of mouse GC taste coding.

"Taste specificity". The above analysis provides one estimate of the number of tastes to which a neuron responds. This fails to provide a rigorous description of the taste-specificity of the neuron's firing, however—it is now well-recognized that the reaching of conclusions regarding differences between responses using only separate tests of each response (e.g., concluding that "because the neuron responds to both X and Y, its responses to X and Y are the same" or that "because the neuron responds significantly to X but not to Y, its responses to X and Y are significantly different") is statistically invalid (Nieuwenhuis, et al., 2011).

We instead tested (as we have using rat data, Li et al., 2013; Piette et al., 2012; Saddaca et al., 2012) whether a single-neuron's responses were "taste specific" *via* direct comparison of the firing rates elicited by the 4 tastes. Specifically, taste-induced firing was divided into four consecutive 500-ms bins, and a mixed-design ANOVA was conducted with taste as the between-subject variable and time as the within-subject variable; a neuron's responses were categorized as taste-specific if either the main effect of taste or the taste X time interaction was significant ($p < 0.01$): the former significant effect indicates simple taste specificity—at least one taste induced an amount of spiking that differed significantly from that driven by at least one other taste; the latter indicates "temporal coding" (in quotes because the suggestion is not that taste identification comes

from analysis of the time-course of firing, but that cortical taste processing is poorly characterized using only overall firing rate averages, see Discussion)—that the time course of the response to one taste was different from the time course of the response to at least one other taste (note that a set of responses could be identical in average rate but differ in time course, in which case the taste main effect would be non-significant while the taste x time interaction would be significant). Post-hoc tests (Tukey's HSD) revealed precisely which responses differed from which.

"Entropy (H)". We employed the oft-used entropy (H) metric as a direct evaluation of the breadth of single-neuron tuning. H was computed as previously described by Smith and Travers (1979) using the following formula (see also Wilson and Lemon, 2013):

$$H = -K \sum_{i=1}^{n} Pi \log Pi,$$

where K is a constant (K = 1.66 for a 4-taste battery), and P is the proportional response to each taste (i). A low H value indicates higher selectivity (H=0 means that a unit responds purely to one taste), whereas a high H value represents broader tuning (H=1 means that a unit responds to all tastes). Taste evoked responses used for entropy analyses were calculated by subtracting mean firing rates of pre-taste delivery (2 seconds) from post-taste taste delivery (2 seconds).

As a set, the above three analyses provide a rich description of GC neuron taste-responsiveness. For instance, a neuron that responds to all tastes equally would have high entropy and broad taste responsiveness, but would likely be responding not to taste quality *per se* but to some other aspect of the stimulus. Accordingly, its firing would almost certainly fail to be deemed taste-specific according to the taste main effect in a 2-way ANOVA.

Finally, it is worth noting that any particular H between 0 and 1 can conceivably be described to represent "broad" or "narrow" coding, depending upon one's perspective. To enhance interpretability of H distributions, we therefore compared our results to those of identical analyses performed on simulated datasets (created based on the real data) made up of units with known breadth.

"Time course of palatability-related responding." Once more taking a cue from our work on rats (e.g., Fontanini et al., 2009; Piette et al., 2012; Sadacca et al., 2012; Li et al., 2016; Sadacca et al., 2016), we used a moving-window analysis to identify time periods in which GC taste responses reflected the hedonic value of the tastes. We first ranked the taste stimuli based on their palatability (see below) from highest to lowest—sucrose>NaCl>citric acid>quinine. We then, for each window of neural firing (window size: 250 ms; step size: 25 ms), performed a (Pearson product-moment) correlation between the firing rates to each taste and the palatability rankings. Because this procedure results in a relatively large number of actual tests, we limited the chances of Type I errors by requiring that the test achieve significance for 3 consecutive bins before responses could be deemed palatability-related.

Taste palatability assessment

To determine the palatability of each of the taste used in this study, mice (N=32; a separate set from those used in the electrophysiology experiment) were mildly water restricted for 3 days (two 30-min periods of access to water per day: one in the morning, and another in the afternoon). On the following day, mice were exposed to one of the tastes (sucrose, NaCl, citric acid, or quinine) for 30 min, and consumption was measured by weight. While our use of these data does not depend on the significance of consumption decisions (in fact, if no structural differences in consumption existed, it would be vanishingly unlikely that there would be significant correlations between the essentially random ranking and neural coding), a one-way ANOVA revealed strong inter-stimulus differences in consumption ($F(3,28) = 32.97$, $p < 0.01$).

Modeling and change-point identification in ensemble firing data

GC taste processing is dynamic—rat cortical responses have been shown to undergo a pair of sudden and coherent firing-rate transitions in the 1.5 sec immediately following taste delivery; the state prior to the first transition is the same for all tastes, reflecting taste 'detection;' the states attained following the first and second transitions are both taste-specific, with the last state further reflecting taste palatability (and both predicting and driving taste behavior in single trials, see Sadacca et al., 2016; Li et al., 2016). In order to detect whether such transitions between states are also facets of mouse cortical taste processing, we performed a simple change-point analysis on ensemble spike data. This analysis is summarized here; for complete details, see Mukherjee et al. (2017).

Trials of ensemble spiking data were categorized in terms of which neuron spiked in each 1-ms bin; an index of 0 corresponded to no spikes from any neuron. If more than one neuron spiked in a time bin—a highly uncommon occurrence, given the relatively low firing rates of GC neurons—we randomly selected one spiking neuron to index that bin (Jones et al., 2007; Sadacca et al., 2016). We then fit a change-point model to the first 1.7s of post taste delivery ensemble activity, describing ensemble firing rate transitions between states as categorical distributions with emissions. We initially considered the possibility that our murine GC data might be best fit by models containing fewer or more than 2 change points. To compare the quality of the fits of the different models to the ensemble spiking data, we computed the Akaike information criterion (AIC) using the formula $AIC = 2*k - 2*LL$, wherein k represents number of parameters and LL is log likelihood of a particular model, and then examined the properties of the identified change points.

As the results of this analysis confirmed the appropriateness of the 3-state (i.e., 2-change point) model (see Results), we constructed a more extensive model constrained on the basis of the rat cortical findings described above: specifically, we constrained the change from state 1 to state 2 (change-point 1, or CP1) to happen within the interval [50 – 600 ms], and constrained the second change-point (CP2) to occur within the interval

[CP1 + 0.2s to 1500ms]. This is equivalent to placing uniform priors over the intervals that define CP1 and CP2, corresponding to the timing of sudden, coherent firing rate transitions in GC ensembles (Jones et al., 2007, Sadacca et al., 2016). With these assumptions, the Expectation-Maximization (EM) algorithm, the most widely used approach to perform inference in such models with latent variables (CP1 and CP2), was employed to fit the change-point model (Bishop, 2016).

Note that to facilitate a central test of this model, the above-described constraints on the timing of state changes are broad and deliberately not centered on the average timing of the transitions as previously observed in rats: specifically, on the basis of our previous work, we predicted CP1 to occur on average at ~200 ms post-delivery, and predicted CP2 to occur on average at ~900 ms post-delivery. If ensemble spiking fails to go through genuinely sudden, coherent firing transitions, any change points identified by the analysis would instead appear (on average) in the middle of the available interval. This result, or any change-point timings, would falsify the prediction that mouse GC ensemble taste responses resemble rat GC ensemble taste data.

Histology

At the end of each experiment, mice were deeply anesthetized and perfused transcardially with 0.9 % saline for 1 minute followed by 4% paraformaldehyde. Brains were extracted and post fixed in 4% paraformaldehyde for 24-48 hours, after which coronal brain slices (60 µm) containing the GC were sectioned on a vibratome. Sections were rinsed 5-6 times over 90 mins (PBS/.3% Triton X-100), mounted on charged glass slides, and cover slipped with mounting medium including DAPI (Vectashield). The placement of electrodes was determined by localizing Dil (a lipophilic dye coated on electrodes during implantation). To visualize electrode bundle locations, bilateral GC sections were viewed by confocal fluorescence microscopy with a Leica Sp5 Spectral confocal microscope/Resonant Scanner with 405 (for DAPI), 546 (Dil dye) and 488 (for GFP) lasers equipped with x/y/z movement stage.

Results

We recorded the spiking of ensembles of single murine gustatory cortical (GC) neurons, using bilaterally implanted electrode bundles, in response to a stimulus battery representing four major taste modalities (sweet: 0.2 M sucrose, salty: 0.1 M sodium-chloride, sour: 0.02 M citric-acid and bitter: 0.001 M quinine) delivered *via* intra oral cannula (15 deliveries of 15 µl).

A total of 185 units were isolated across 10 sessions in 6 mice—4 mice received 2 sessions each (in which case sessions were recorded from separate DV locations in the GC; see material and methods). Our recordings spanned much of the GC region (AP Bregma +1.6 to 0.0; DV 2.25 – 3.25 mm from the surface of the brain; see Figure 1) receiving input from taste thalamus (Chen et al., 2011; Fletcher et al., 2017) or from the amygdala (Matyas et al., 2014); prior work has shown this region to be important for taste behavior and learning in mice (Neseliler et al., 2011).

Basic characterization of taste evoked responses in the gustatory cortex of mice

Figure 2 presents raster plots and associated PTSHs of the taste responses of three simultaneously recorded GC neurons. The first two are regularly spiking (putative) pyramidal neurons and the third is a fast-spiking (putative) inhibitory interneuron. Each neuron's responses were significantly (see Methods) taste-specific: Unit 1 responded to all 4 tastes, but responded more strongly to NaCl and sucrose than to the remaining tastes; Unit 2, on the other hand, responded strongly to sucrose, citric acid, and quinine, but far less to NaCl; Unit 3, meanwhile, was inhibited to differing degrees and for differing lengths of interval by all 4 tastes.

Even the most basic examination of these responses (i.e., analyzing average firing rates, and ignoring differences in temporal coding) revealed (consistent with what has been reported in awake rats, e.g., Piette et al., 2012; Moran and Katz, 2014), that a large percentage (just under 2/3) of mouse GC neurons respond to taste stimulation (significant paired t-tests comparing pre- to post-stimulus firing across all trials summed across tastes, Figure 3A); excitatory responses (enhanced firing) outnumbered inhibitory (reduced firing) by almost 3 to 1. Using ANOVAs to directly compare each neuron's response to different tastes, and including time as a 2nd factor, we were able to identify an almost identical percentage of neurons as being "taste neurons" (i.e., responding distinctly to at least one taste, see Methods and Figure 3C). While these two analyses will not necessarily identify precisely the same neurons (see Methods), together they suggest that the vast majority of "taste responses" in mouse GC are truly taste-related, as opposed to reflecting somatosensory or general cognitive factors.

While taste-specific, these responses were broad—significant firing rate modulations in individual neurons were seldom restricted to only one, or even two, of the four basic tastes delivered. Had they been narrow, then the rate of significant responses to each individual

taste (determined using simple t-tests, as above, applied to each individual PSTH) would be expected to be around ¼ of this 66% (that is, we'd expect ~16% of the neurons to have sucrose responses, another ~16% to have NaCl responses, etc). A far higher percentage of neurons responded to each taste, however (Figure 3B), a result that suggested that most taste neurons in mouse GC must respond to > 1 taste on average.

We performed multiple convergent tests of this conclusion. First, we directly analyzed the number of tastes that evoked significant responses in each individual neuron (by pre- vs post-stimulus t-tests). This analysis revealed that 28.6% of our mouse GC neurons responded significantly to one taste; 25.6% responded to two tastes, 16.8% to three tastes, and 14.1% to all four tastes (Figure 4A). While it is inappropriate to reach conclusions concerning taste specificity from this method (which does not directly compare responses to different tastes, see Methods), these results confirm that the majority of GC neurons that respond to taste stimulation respond to > 1 taste.

We went on to calculate response entropy (H) for each neuron, using standard techniques (Smith and Travers., 1979; Samuelsen et al., 2013); low H values indicate narrowly responsive neurons, and high H values indicate broadly tuned neurons. The distribution for our neural sample proved to be highly positively skewed, with the vast majority of GC neurons' H values suggesting broad responsiveness; the distribution was similar when only neurons identified as responding in a taste-specific manner were included (Figure 4B).

To enhance the interpretability of this result (see Methods), we plotted the distribution of entropies against the H values of a simulated set of neurons that all responded to only one taste: this distribution is significantly different from the distribution of the real data ($X^2 = 82.75$, $p < 0.01$) which most resembles (according to Kullback-Leibler divergence) data from neural data simulated to have responses to 3 to 4 tastes (Figure 4C).

Dynamics of taste-evoked responses in mice GC

The above data suggest that GC taste neurons are broadly tuned "coarse coders," responding distinctly to multiple tastes; as such, they are consistent with previous reports of taste responses in rat GC (Yamamoto et al., 1985; Bahar et al., 2004; Fontanini and Katz., 2006; Jones et al., 2007; Piette et al., 2012; Samuelsen et al., 2013), and with calcium imaging data from mouse GC (Fletcher et al., 2017; but see Chen et al., 2011). But the prior work on rats further demonstrates that such analyses inadequately describe GC taste responses, in that they ignore meaningful response changes that occur across the first 1.5s of post-stimulus time (the period leading up to the making of consumption decisions and production of consumption-related behaviors, see Grill & Norgren, 1978; Travers and Norgren., 1986; Li et al., 2016). The complete range of the information carried in rat GC taste responses can be appreciated only when reliable, phasic modulations of firing rate—the temporal dimension of taste responses—are considered (Katz et al., 2001;

Fontanini & Katz, 2006; Piette et al., 2012; Sadacca et al., 2012; Maier & Katz, 2013; Li et al., 2016; Baez-Santiago et al., 2016).

Scrutiny of taste PSTHs suggests the presence of interpretable firing-rate dynamics, with response magnitudes changing through time in taste-specific manners. An example is shown in Figure 5A—a mouse GC neuron that responded strongly to NaCl during the 1st post-delivery second only, and strongly to citric acid during the 2nd post-delivery second only (note that when this pattern of firing is averaged across time, the neuron incorrectly registers as being responsive to quinine only, once again demonstrating the inadequacy of that earlier analysis for the purposes of completely characterizing the taste-specificity of firing).

To more rigorously evaluate the temporal evolution of these responses in relation to the sensory and psychological properties of taste perception, we first ascertained mouse behavioral preferences for our battery of four tastes (which differed in both chemical identity and palatability, sucrose and sodium-chloride representing palatable tastes and citric acid and quinine representing non-palatable tastes) using a single-bottle consumption test. We then correlated this vector of palatabilities with the vector of firing rates to the same battery of tastes in small bins of the 2-sec response epoch (using a moving-window analysis as explained in the Methods and used previously in Fontanini et al., 2009; Piette et al., 2012; Sadacca et al., 2012; Li et al., 2016; Sadacca et al., 2016).

An example of the result of this analysis is shown in Figure 5A2 (with the taste preference data presented as an inset): for this single neuron, firing did not become significantly palatability-related (green dots) until several hundred msec after the onset of taste responsiveness, and reached a peak of palatability-relatedness a full sec after taste delivery; inspection of Figure 5A1 reveals that the neuron's response was taste-specific prior to the emergence of palatability-relatedness, but that firing rates shifted beginning 0.5 sec later such that the order of response magnitudes came to reflect palatability (in this case the ordering was "aversive high," which appeared with approximately the same frequency in our neural sample as "aversive low").

Figure 5B, which presents the results of this analysis performed upon the entire data set, confirms the representativeness of the example: the incidence of taste specificity rises almost immediately following taste stimulus delivery, and approaches peak levels as early as 500 ms into the response; palatability relatedness, on the other hand, rises more slowly, beginning to trend upward ~500 ms after stimulus delivery and approaching a peak ~1000 ms into the response.

We performed one further test of this result, analyzing the distinctiveness of different subsets of taste responses for each neuron at each point in response time; "distinctiveness" was quantified in terms of normalized Euclidean distances separating two taste responses in a multi-dimensional scaling solution. Given the above results, we predicted that the distinctiveness of individual pairs of tastes would rise quickly, but that the distinctiveness of palatability differences—that is, comparisons of the averaged

responses to the palatable tastes (sucrose and NaCl) to the averaged responses to the aversive tastes (quinine and citric acid)—would emerge only later. Figure 5C reveals that this is precisely what we observed: the distinctiveness of codes for sucrose and NaCl (yellow line ± SE) rose quickly in post-delivery time, as did the distinctiveness of codes for quinine and citric acid (beige line ± SE); the rise in the distinctiveness of palatabilities (green line ± SE), meanwhile, was delayed. Note as well that following the rise of palatability distinctiveness, the distinctiveness of individual "same-palatability" taste pairs fell precipitously, confirming that general taste-specificity becomes refined across time into palatability-relatedness.

Thus, we conclude that mouse GC codes taste properties sequentially across 1.5 seconds of post-stimulus time, with taste-specificity appearing prior to palatability-relatedness. Ancillary analysis confirms that many individual neurons respond distinctly in the two epochs, coding both taste identity early and taste palatability late. In fact, 50% of the neurons that produce significantly taste-specific firing also produce significantly palatability-related firing (as in the example neuron shown in Figure 5a).

Ensemble properties of murine cortical taste dynamics

Having established the existence of reliable, interpretable single-neuron dynamics in mouse GC, we moved on to asking whether these single-neuron dynamics are in fact reflections of coherent ensemble activity (as they are in rats, see Sadacca et al., 2016). As we have done with rat data (Mukherjee et al., 2017), we applied change-point (CP) modeling (see Methods) procedures to datasets comprised of simultaneously-recorded neural ensembles, to test whether firing rate transitions between epochs are: 1) coherent between neurons; 2) sudden; and 3) trial-specific in latency.

We compared our ability to model the data using 2 CPs (the predicted model given the above results and previous work on rats) to that achieved using models with fewer or more CPs. Initial assessment of the quality of model fit making use of the Akaike information criterion (AIC) confirmed that murine GC ensemble taste data are typically well characterized as going through a set of three states separated by two CPs (2 sudden transitions of firing that were coherent across simultaneously-recorded neural ensembles). While in a subset of instances a 3-CP model fit equally well, scrutiny of these successful 3-CP fits revealed that, in over half of the trials, multiple CPs were clustered with minimal time separations—they were essentially 2-CP solutions with one of the CPs reduplicated. Similar results were observed in a subset of datasets in which the fit of a 4-CP model was examined. Clearly, mouse GC taste responses are best described as going through a sequence of 3 firing-rate "states" separated by sudden, coherent ensemble firing-rate transitions.

Our analysis of the data as characterized by the 2-CP model demonstrates further features of the taste code in mouse GC. Figure 6A shows an example of 3 sucrose trials; a one-way ANOVA revealed that the palatability correlation varied with Epoch ($F = 24.36$, $p < 0.01$), and post-hoc comparisons revealed that this significance is largely driven by the fact that the correlation with palatability is significantly higher following the second transition than before ($p < .05$). The fact that palatability correlations are modestly higher following the first transition than before reflects the simple fact that the very earliest 100-200ms of GC responses (i.e., the brief period preceding even the 1st transition) are, as they are in rats, totally non-specific; almost any taste specificity will enhance correlations with palatability beyond those chance correlations observed with non-specific firing.

The average transition times for CP1 and CP2 occurred at ~190 ms and ~800 ms, respectively (Figure 6C). Note that these average transition times differed distinctly from the time-point that represented the middle of the available intervals (i.e., 325 for CP1 and 925ms for CP2; see Methods). This finding is inconsistent with the hypothesis that the CPs are simply artifacts of the procedure itself; rather, these latencies are good matches for our prior rat data, and for our single-neuron results (Fig 5D), and confirm our expectation that mouse GC ensembles undergo fairly sudden and coherent shifts in firing while responding to tastes.

These results suggest that even dynamic analysis of single-neuron taste responses in mouse GC, as described above, fail to completely characterize taste processing. Rather than being independent elements, single-neuron responses are likely reflections of population coding—an unsurprising fact given the mesoscopic (intracortical connectivity) and macro-scopic (between-region feedback) circuitry involved in taste.

Spatial analysis of murine cortical taste response properties

GC is a distributed, inhomogeneous region that can be subdivided according to cytoarchitectural and connectivity criteria in the dorsal-ventral (into granular, dysgranular and agranular regions) and anterior-posterior axes (Allen et al., 1991; Maffei et al., 2012). One subset of the imaging literature has suggested that mouse cortical taste coding, unlike that of rat (Accolla et al., 2007), is cleanly gustotopic (Chen et al., 2011; Wang et al., 2018), while other subsets suggest otherwise (Fletcher et al., 2017; Lavi et al., 2018).

To explore the potential spatial dependencies of GC taste coding using electrophysiology (which is far more sensitive to subtle responses), we compared taste-evoked firing along the two primary axes of GC. In the dorsal-ventral dimension we were able to look within-subject, as our electrode bundles could be driven ventrally between tasting sessions. Figure 7 shows a pair of example neurons recorded from dorsal GC, and a second pair recorded from ventral GC in the same mouse. It can be seen that each of these responses are quite broad, suggesting basic similarities between dorsal and ventral GC.

Closer analysis confirmed the similarity of different recording depths. Analysis of the entire sample divided into dorsal and ventral recordings revealed no striking differences in breadth of responsiveness, measured either in terms of number of tastes responded to (Figure 8a, $X^2 = 1.15$, $p = 0.885$) or response entropy (Figure 8b; $X^2 < 1$). The magnitudes of taste specificity revealed by ANOVA was similar across dorsal and ventral neurons (Fig. 8C; $F < 1$), and the pattern of how many neurons responded to which taste did not differ significantly between subregion (Figure 8D); in both dorsal and ventral GC, single neurons were more likely to respond to both palatable and aversive neurons than either alone (data not shown). Finally, dorsal and ventral neural samples showed similar time-courses of response evolution from quality to palatability, measured in terms of the number of neurons showing such responses at each time point (Figure 8E1-2).

In the anterior-posterior dimension, our results were analogous. We compared taste responses between bregma +1.6 and bregma 0.0, treating everything forward of 0.8 as "anterior." This analysis also revealed no aspects of taste coding that varied notably with anatomical location: we saw no significant differences between anterior/posterior breadth of responsiveness, measured either in terms of number of tastes responded to (Figure 9A, $X^2 = 5.51$, $p = 0.239$) or response entropy (Figure 9B; $X^2 < 1$); furthermore, neurons from anterior and posterior GC subdivisions had similar magnitudes of taste specificity (Figure 9C; $F < 1$), similar patterns of how many neurons responded to each taste (Figure 9D), and similar time-courses of response evolution from quality to palatability (Figure 9E1-2).

Together these results suggest that the details of taste coding are relatively insensitive to anatomical location within mouse GC – neurons across the anterior-posterior and dorsal-ventral axes code all taste modalities in a broad and temporally complex manner. Of course, the lack of significant difference does not equal rigorously identified "sameness," and the possibility remains that subtle differences between anatomical subregions (or between species, for that matter) remain to be identified. Nonetheless, these analyses fail to reveal major differences in taste coding across the breadth of mouse GC.

Discussion

Mice have become the most common non-human mammalian species studied by neuroscientists—a fact that can no doubt be attributed to the accessibility of mouse genetics, which allows researchers to, with (relative) ease, study the underlying molecular mechanisms of cellular, network, and behavioral phenomena (Stevens, 1996; Kandel et al., 2014). As the sense with (arguably) the tightest link to behavior and learning (Carleton et al., 2010; Maffei et al., 2012; Katz & Sadacca, 2010), taste is a particularly good system with which to study these topics in a unified manner. Furthermore, this work can take advantage of the extensive progress that has been made toward understanding key principles of taste coding in awake rats (Accolla et al., 2007; Bahar et al., 2004; Fontanini and Katz., 2006; Jones et al., 2007; Katz et al., 2001; Li et al., 2016; Moran & Katz., 2014; Sadacca et al., 2012; Samuelsen et al., 2012). It is somewhat surprising, therefore, that there has been almost no electrophysiological work done on mouse cortical taste coding, and that the imaging studies performed thus far have failed to provide consensus on basic features of gustatory sensory coding (Chen et al., 2011; Fletcher et al., 2017; Lavi et al., 2018).

In fact, while electrophysiological responses to stimuli including tastes have been examined in anesthetized mice (Wilson and Lemon, 2013), the current study represents the first thorough investigation of single-neuron spiking responses to a broad battery of taste stimuli by primary gustatory cortical (GC) neurons in awake mice (but see Kusamoto-Yoshida et al, 2015). By delivering a battery of four basic tastes (sweet, salty, sour and bitter) directly to the tongue of freely moving mice while making recordings from a multi-electrode bundle designed to record the activity of small ensembles of single neurons, we show that mouse GC codes taste in a largely non-sparse manner: approximately 2/3 of recorded GC responses conveyed information about taste identity; by and large, these responses were broadly tuned—over half of the recorded neurons responded to > 1 taste, and over half of taste neurons produced firing patterns that were distinctive for 3 of 4 tastes.

But the taste responses of murine GC neurons, while broad, are not unstructured; rather, they evolve in a characterizable way across 1-1.5 seconds. We were able to identify separate “epochs” of GC responses related to the physiochemical and psychological properties of the tastes in our stimulus battery. A large portion (50%) of the recorded neurons coded stimulus identity and stimulus palatability sequentially, rather than being active in only one coding epoch; in fact, transitions between response epochs could be observed in single trials using ensemble statistics. These results suggest that the processing of quality and palatability is likely not performed by independent neural ensembles.

Our study provides a foundation for comparative analysis of mice and rat GC taste processing. Although the anatomies of the two species’ taste systems are thought to be similar, little work has been done comparing taste coding between the two species. In all of our current results, we observed a striking similarity between mouse cortical taste

coding and that extensively described in rat data (Accolla et al., 2007; Bahar et al., 2004; Fontanini and Katz., 2006; Jones et al., 2007; Piette et al., 2012; Sadacca et al., 2012; Samuelsen et al., 2013; Yamamoto et al., 1985;). Both species code tastes broadly, and these codes reflect identity and taste palatability in separate, sequential epochs. It may well be that differences will emerge with regard to the impact of taste learning on neural coding (which we will examine in the future).

Note that these data do not address the question of whether the coding of taste is necessarily "temporal coding" *per se* (although see Di Lorenzo et al., 2009; Erickson et al., 1994; Hallock and Di Lorenzo, 2006; Lemon and Smith, 2006): mouse GC taste responses become taste-specific at approximately 0.15-0.2 sec after taste delivery, a latency that accords well with the absolute minimum behavioral reaction times to tastes (Halpern and Tapper, 1968, 1971; Perez et al., 2013); firing at that latency is best described as "across-fiber patterns" (although not as "labeled lines," see Erickson, 1963, 1982). Rather, our data suggest that the term "taste coding" far under-describes the work that GC is involved in, in that GC responses chart the transformation of taste information into an action (i.e., palatability) code. Evidence supporting this conception comes from rat studies showing that the onset of palatability-related firing both predicts (Sadacca et al., 2016) and drives (Li et al., 2016) the onset of taste behavior.

It was important that we extend the above-described analyses into the spatial domain (a possibility that has not been addressed in our work on rat GC), probing for possible differences in how dorsal/ventral and anterior/posterior sub regions of GC code tastes, because: 1) GC subregions form distinct connections with other brain regions along the dorsal/ventral and anterior/posterior axes (Allen et al., 1991; Haley, et al., 2016; Maffei et al., 2012); and 2) the literature on imaging of mouse GC fails to support consistent conclusions on the matter (Chen et al., 2011; Livneh et al., 2016; Fletcher et al., 2017; Lavi et al., 2018). Our comparisons revealed remarkably little spatial variance of coding, consistent with Fletcher et al (2017; see also Accolla et al., 2007 and Lavi et al., 2018)—neurons across the heart of GC produced similarly broad, temporally complex taste responses.

This invariance in the face of non-uniform input—most notably, dorsal GC receives mainly thalamic input whereas ventral GC receives mainly amygdala input, the latter of which is important for palatability coding (Piette et al., 2012)—suggests that GC taste responses are to a large extent a function of distributed network processing, rather than of direct sensory or effective input. This interpretation is supported by the very finding that GC neurons code multiple aspects of tastes in a temporally distributed fashion, which suggests convergence of pathways, and population coding analysis that reveal the temporal codes to be a reliable sequence of coherent network states (see Grossman et al., 2008; Jones et al., 2007; Moran & Katz, 2014; Sadacca et al., 2016).

Together our results shed a new light on the structure of taste coding in mice. They show that GC neurons are broadly tuned, coding multiple tastes and multiple aspects of taste processing (taste identity and palatability) in time-varying responses, and that these

responses are distributed through a broad spatial extent of GC; cortical network processing is distributed, rather than being separated out into spatial subregions. At the largest “big picture” level, these results suggest that the functional unit of sensory processing in GC is ensembles composed of neurons that are responsive to multiple tastes, in which properties of the processing emerge transiently in specific time epochs.

References

Allen GV, Saper CB, Hurley KM, Cechetto DF (1991) Organization of visceral and limbic connections in the insular cortex of the rat. J Comp Neurol 311:1-16.

Accolla R, Bathellier B, Petersen CC, Carleton A (2007) Differential spatial representation of taste modalities in the rat gustatory cortex. J Neurosci 27:1396-1404.

Bahar A, Dudai Y, Ahissar E (2004) Neural signature of taste familiarity in the gustatory cortex of the freely behaving rat. J Neurophysiol 92:3298-3308.

Baez-Santiago MA, Reid EE, Moran A, Maier JX, Marrero-Garcia Y, Katz DB (2016) Dynamic taste responses of parabrachial pontine neurons in awake rats. J Neurophysiol 115:1314-1323.

Bartho P, Hirase H, Monconduit L, Zugaro M, Harris KD, Buzsaki G (2004) Characterization of neocortical principal cells and interneurons by network interactions and extracellular features. J Neurophysiol 92:600-608.

Carleton A, Accolla R, Simon SA (2010) Coding in the mammalian gustatory system. Trends Neurosci 33:326-334.

Chen X, Gabitto M, Peng Y, Ryba NJ, Zuker CS (2011) A gustotopic map of taste qualities in the mammalian brain. Science 333:1262-1266.

Di Lorenzo PM, Platt D, Victor JD (2009) Information processing in the parabrachial nucleus of the pons. Ann N Y Acad Sci 1170:365-371.

Erickson RP (1963) Sensory neural patterns and gustation. Olfaction and taste 1:205-213.

Erickson RP (1982) Studies on the perception of taste: do primaries exist? Physiol Behav 28:57-62.

Erickson RP, Di Lorenzo PM, Woodbury MA (1994) Classification of taste responses in brain stem: membership in fuzzy sets. J Neurophysiol 71:2139-2150.

Fletcher ML, Ogg MC, Lu L, Ogg RJ, Boughter JD, Jr. (2017) Overlapping Representation of Primary Tastes in a Defined Region of the Gustatory Cortex. J Neurosci 37:7595-7605.

Fontanini A, Katz DB (2006) State-dependent modulation of time-varying gustatory responses. J Neurophysiol 96:3183-3193.

Grossman SE, Fontanini A, Wieskopf JS, Katz DB (2008) Learning-related plasticity of temporal coding in simultaneously recorded amygdala-cortical ensembles. J Neurosci 28:2864-2873.

Halpern BP, Tapper DN (1971) Taste stimuli: quality coding time. Science 171:1256-1258.

Hallock RM, Di Lorenzo PM (2006) Temporal coding in the gustatory system. Neurosci Biobehav Rev 30:1145-1160.

Haslinger R, Ulbert I, Moore CI, Brown EN, Devor A (2006) Analysis of LFP phase predicts sensory response of barrel cortex. J Neurophysiol 96:1658-1663.

Ji D, Wilson MA (2007) Coordinated memory replay in the visual cortex and hippocampus during sleep. Nat Neurosci 10:100-107.

Jones LM, Fontanini A, Sadacca BF, Miller P, Katz DB (2007) Natural stimuli evoke dynamic sequences of states in sensory cortical ensembles. Proc Natl Acad Sci U S A 104:18772-18777.

Kandel ER, Dudai Y, Mayford MR (2014) The molecular and systems biology of memory. Cell 157:163-186.
Katz DB, Simon SA, Nicolelis MA (2001) Dynamic and multimodal responses of gustatory cortical neurons in awake rats. J Neurosci 21:4478-4489.
Kusumoto-Yoshida I, Liu H, Chen BT, Fontanini A, Bonci A (2015) Central role for the insular cortex in mediating conditioned responses to anticipatory cues. Proc Natl Acad Sci U S A 112:1190-1195.
Lavi K, Jacobson GA, Rosenblum K, Luthi A (2018) Encoding of Conditioned Taste Aversion in Cortico-Amygdala Circuits. Cell Rep 24:278-283.
Lemon, C. H., & Smith, D. V. (2006). Influence of response variability on the coding performance of central gustatory neurons. J Neurosci, 26(28), 7433-7443.
Li JX, Yoshida T, Monk KJ, Katz DB (2013) Lateral hypothalamus contains two types of palatability-related taste responses with distinct dynamics. J Neurosci 33:9462-9473.
Li JX, Maier JX, Reid EE, Katz DB (2016) Sensory Cortical Activity Is Related to the Selection of a Rhythmic Motor Action Pattern. J Neurosci 36:5596-5607.
Maffei A, Haley M, Fontanini A (2012) Neural processing of gustatory information in insular circuits. Curr Opin Neurobiol 22:709-716.
Matyas F, Lee J, Shin HS, Acsady L (2014) The fear circuit of the mouse forebrain: connections between the mediodorsal thalamus, frontal cortices and basolateral amygdala. Eur J Neurosci 39:1810-1823.
Moran A, Katz DB (2014) Sensory cortical population dynamics uniquely track behavior across learning and extinction. J Neurosci 34:1248-1257.
Neseliler S, Narayanan D, Fortis-Santiago Y, Katz DB, Birren SJ (2011) Genetically induced cholinergic hyper-innervation enhances taste learning. Front Syst Neurosci 5:97.
Peng Y, Gillis-Smith S, Jin H, Trankner D, Ryba NJ, Zuker CS (2015) Sweet and bitter taste in the brain of awake behaving animals. Nature 527:512-515.
Perez IO, Villavicencio M, Simon SA, Gutierrez R (2013) Speed and accuracy of taste identification and palatability: impact of learning, reward expectancy, and consummatory licking. Am J Physiol Regul Integr Comp Physiol 305:R252-270.
Piette CE, Baez-Santiago MA, Reid EE, Katz DB, Moran A (2012) Inactivation of basolateral amygdala specifically eliminates palatability-related information in cortical sensory responses. J Neurosci 32:9981-9991.
Sadacca BF, Rothwax JT, Katz DB (2012) Sodium concentration coding gives way to evaluative coding in cortex and amygdala. J Neurosci 32:9999-10011.
Sadacca BF, Mukherjee N, Vladusich T, Li JX, Katz DB, Miller P (2016) The Behavioral Relevance of Cortical Neural Ensemble Responses Emerges Suddenly. J Neurosci 36:655-669.
Samuelsen CL, Gardner MP, Fontanini A (2012) Effects of cue-triggered expectation on cortical processing of taste. Neuron 74:410-422.
Samuelsen CL, Gardner MP, Fontanini A (2013) Thalamic contribution to cortical processing of taste and expectation. J Neurosci 33:1815-1827.
Smith DV, Travers JB (1979) A metric for the breadth of tuning of gustatory neurons. Chem Senses 4:215–229.

Sirota A, Montgomery S, Fujisawa S, Isomura Y, Zugaro M, Buzsaki G (2008) Entrainment of neocortical neurons and gamma oscillations by the hippocampal theta rhythm. Neuron 60:683-697.

Stevens CF (1996) Spatial learning and memory: the beginning of a dream. Cell 87:1147-1148.

Tapper DN, Halpern BP (1968) Taste stimuli: a behavioral categorization. Science 161:708-710.

Wilson DM, Lemon CH (2013) Modulation of central gustatory coding by temperature. Journal of neurophysiology 110:1117-1129.

Yamamoto T, Yuyama N, Kato T, Kawamura Y (1985) Gustatory responses of cortical neurons in rats. II. Information processing of taste quality. J Neurophysiol 53:1356-1369.

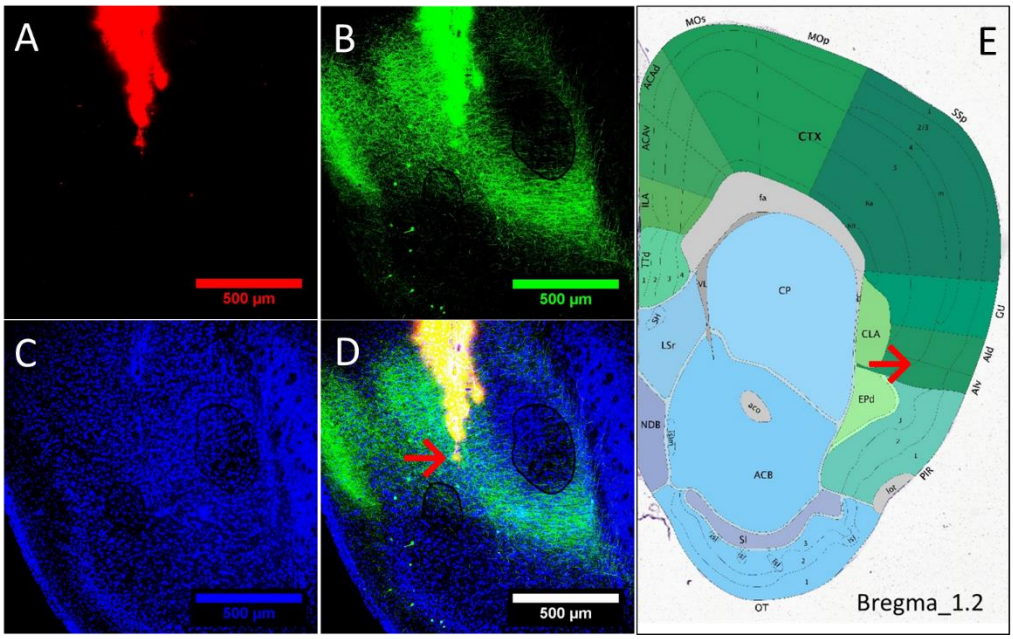

Figure 1. Localization of electrode bundles in mouse GC. **A**. To determine the recording site in GC, electrode bundles were coated with Di-I (a red fluorescent tracer) which later showed the track traveled by the multielectrode array in GC (in a mouse that received two recording sessions, see Methods). **B**. To assist the separation between dorsal and ventral subregions of GC, BLA was infected with AAV2/5::GFP; resultant GFP-labeled axons were then visible in ventral GC. **C** Background staining of the same slice with DAPI (a nonspecific nuclear dye). **D**. In a triple-labeled slice, an arrow indicates the final location of the tips of the electrodes. **E**. A schematic of this slice location (Alan mouse brain atlas, P56, coronal) shows the final location of the electrode to be in ventral and anterior GC.

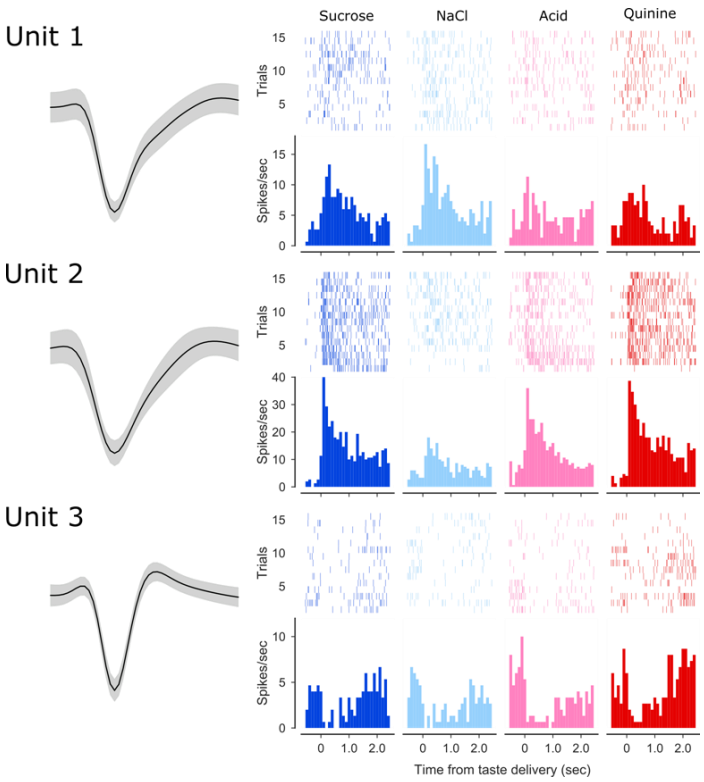

Figure 2. Simultaneously recorded gustatory cortex neurons. The left column shows the average action potential waveforms (surrounded by confidence intervals) for three neurons recorded simultaneously from the same electrode bundle. The remaining four columns show the responses of these neurons to sweet (sucrose), salty (sodium chloride), sour (citric acid) and bitter (quinine) tastes. The top half of each response display is spike time raster plots (each row is a single trial, and each dot is an action potential), below which are associated PTSHs (firing rate in spike/second in the y-axes; time post-stimulus in the x-axes). Each neuron's responses were taste-specific (see Methods), and each individual neuron responded distinctly.

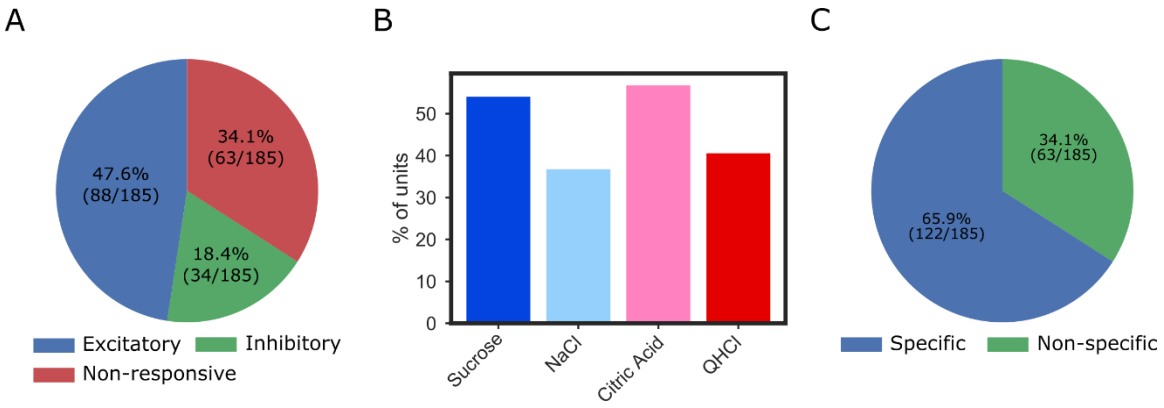

Figure 3. **Mouse GC neurons respond to tastes**. **A.** A pie chart showing the percentage and distribution of GC neurons that produced excitatory or inhibitory responses to taste stimulation. **B**. Similar percentages of mouse GC neurons respond to sweet, salty, sour, and bitter tastes; at least 35% of the sample responded to each taste. **C**. 2-way within-neuron ANOVAs comparing responses to the different tastes as a function of time (taste x time, $p<0.01$) revealed that the majority of mouse GC neuron taste responses were also taste-specific (i.e., different for different tastes).

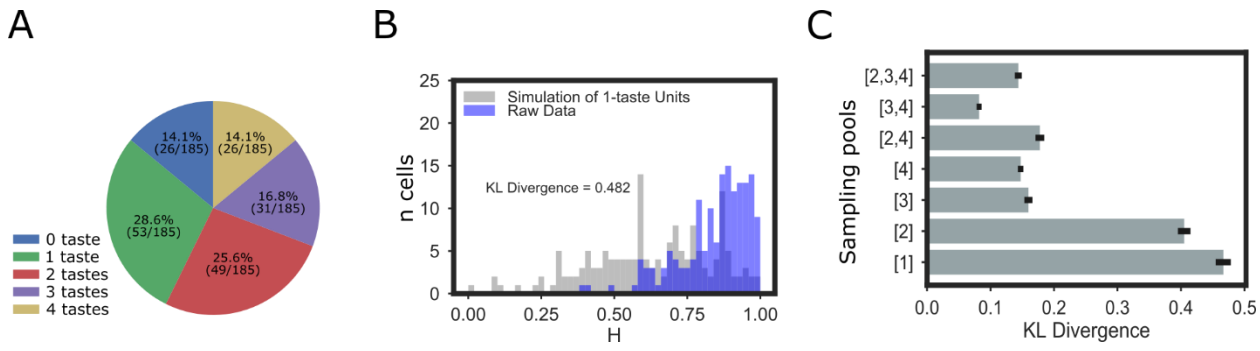

Figure 4. **GC neurons code tastes broadly**. **A.** Independent paired t-tests comparing pre- and post-taste firing rates reveal that the majority of mouse GC neurons respond more than one taste (even when totally non-responsive neurons are included in the comparison). **B.** The distribution of the breadth of taste coding (i.e., entropy [H], x-axis) in GC neurons (purple bars, y-axis = 159 of neurons) is highly skewed toward broad tuning (a low H indicates narrowly responsive neuron and a high H indicates a neuron responsive to several tastes). Overlain (grey bars) is the distribution of response entropies for an equivalently-sized set of simulated units which respond to only one taste. The difference of the two distributions was calculated using the Kullback-Leibler (KL) divergence, and was highly significant according to a X^2 test conducted on the data. . **C**. The KL divergences between the collected data and a range of simulated datasets in which units responded to particular numbers of tastes.

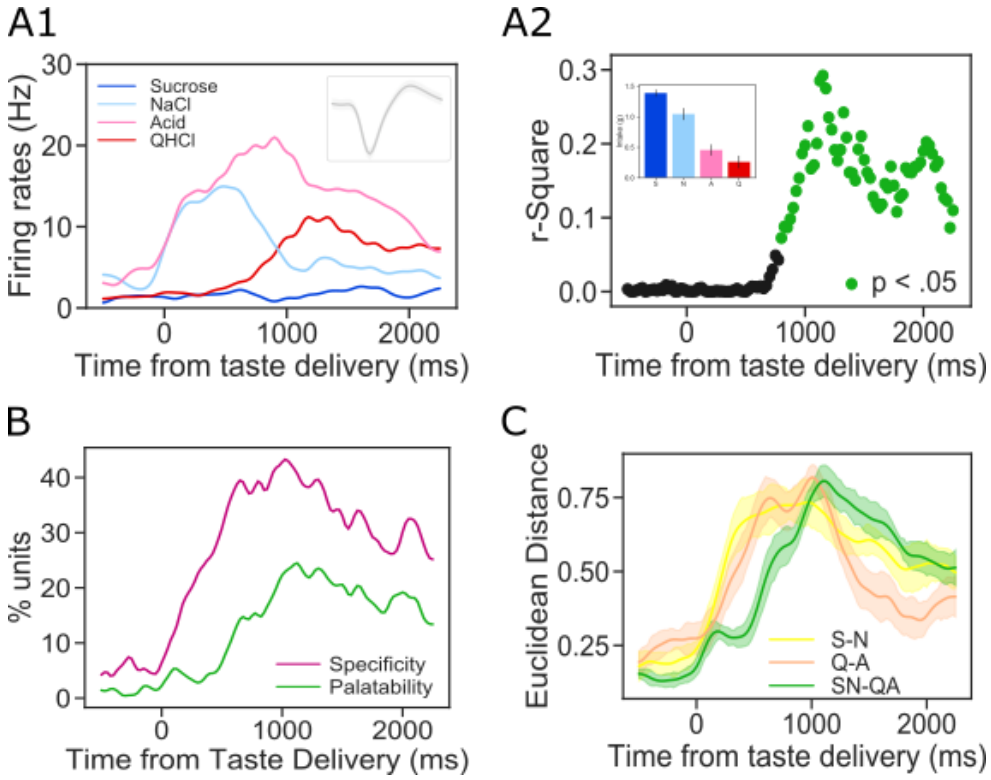

Figure 5. Murine GC responses evolve through successive epochs of taste quality and taste palatability coding. **A1**: Overlain PSTHs (y-axis, firing rate; x-axis, time post-stimulus) from a representative GC neuron that responded significantly to all tastes but sucrose [S]. **A2**: Moving window analysis of the correlation (R-squared, y-axis) between firing rates and taste palatability (determined by taste intake, see inset) for the neuron shown in Panel A1. Green dots denote significantly non-zero correlations. **B**. Percentages of the entire sample of GC responses that show significant taste specificity (magenta) and palatability-relatedness (green). Taste specificity starts to rise soon after taste delivery, and peaks at 500ms; in contrast, palatability-related firing appears only following a delay (~500ms), and peaks at ~1 second post-stimulation. **C**. Response differences (Euclidean separation in multi-dimensional scaling solutions, see methods for details) between same-palatability tastes qualities (S-N and Q-A) emerge soon after stimulus delivery; between-palatability differences, on the other hand (SN-QA) emerge later, confirming that identity-related activity is followed by palatability-related firing.

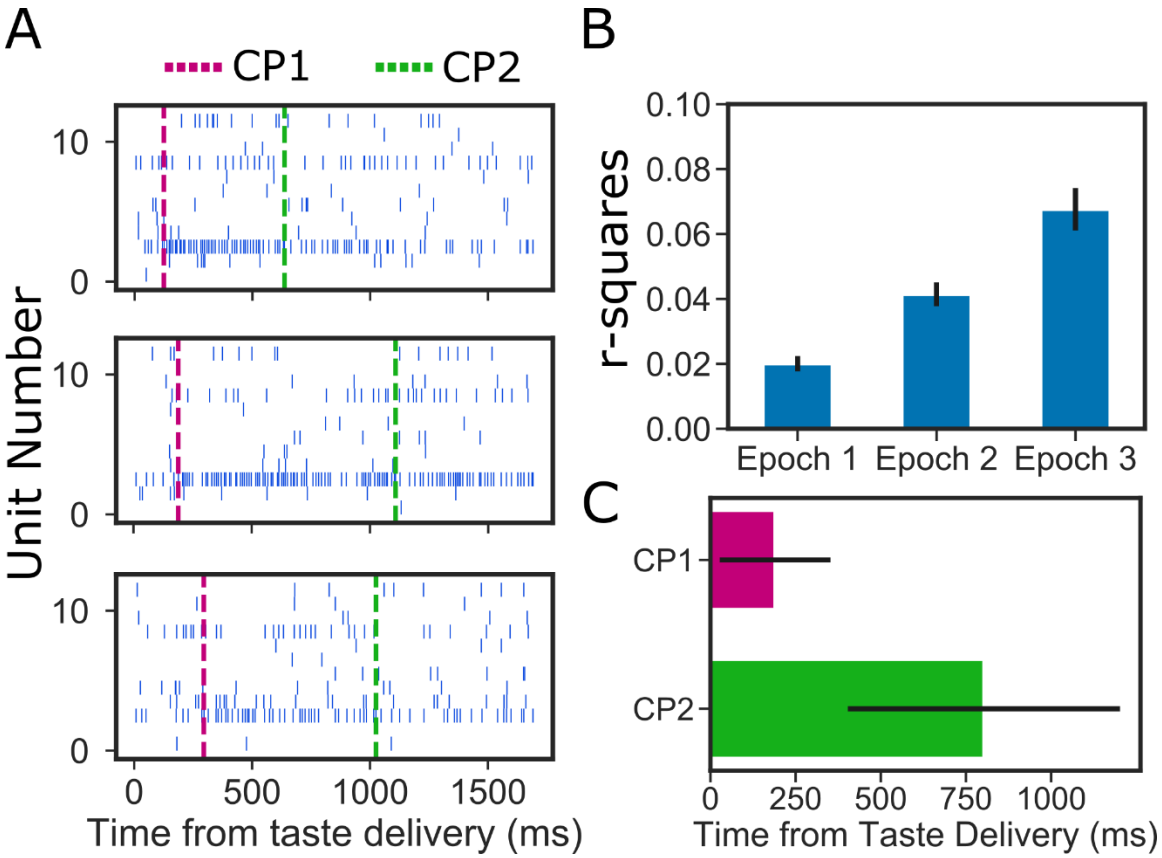

Figure 6. The epochs of mouse cortical taste responses reflect coherent state sequences in GC ensembles. **A.** Representative single trials of the response of one GC ensemble (one neuron/row; hash marks = individual action potentials) to the taste of sucrose, revealing sudden, simultaneous changes in firing rates in several neurons. Magenta and green dashed lines indicate the first switch point (CP1: from taste detection to identity) and second switch point (CP2: from taste identity to palatability), respectively. **B.** Correlations between mean firing rates and palatability for each of the three states, demonstrate, consistent with our hypotheses and work on rat GC, that palatability coding is achieved with state 3, and that taste-specificity (which necessarily connotes a basic level of non-zero palatability coding) is achieved with state 2. **C**. Average state-to-state transition times across all trials revealed through switch point analysis.

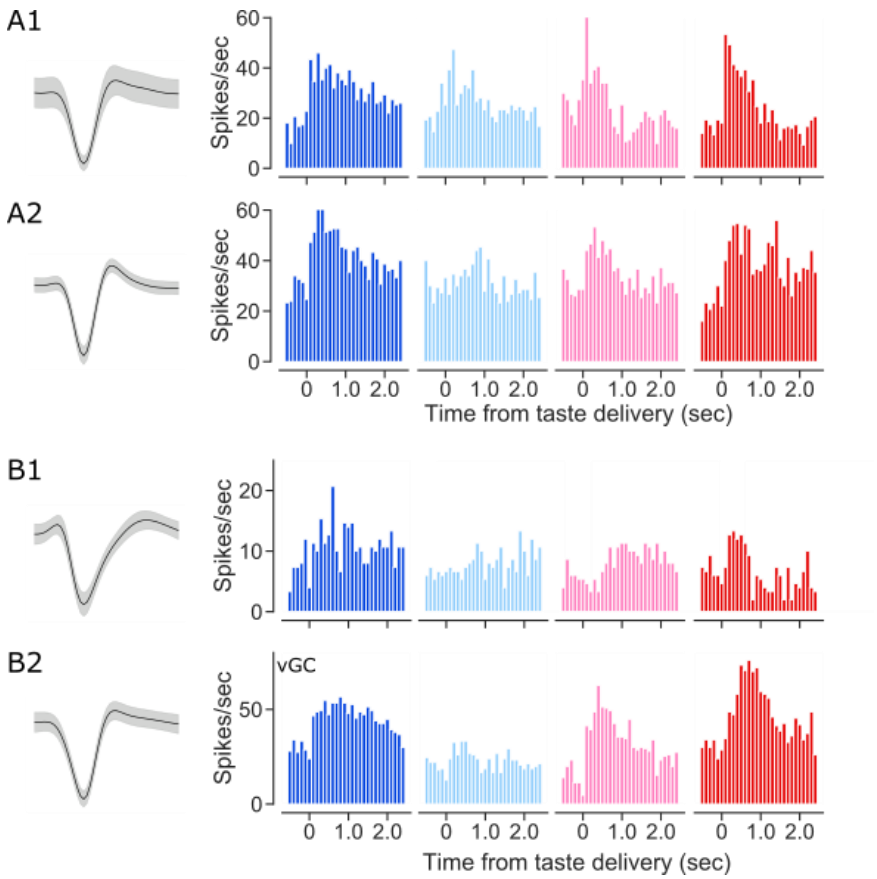

Figure 7. **Broadly-responsive ensembles of GC neurons can be recorded from dorsal (A1, A2) and ventral (B1, B2) GC of the same mouse**. **A1-A2**. Representative neurons (wave shapes and PTSHs, conventions as for Figure 2) recorded in dorsal GC. **B1-B2**. Representative neurons recorded from the same mouse in a 2nd session.

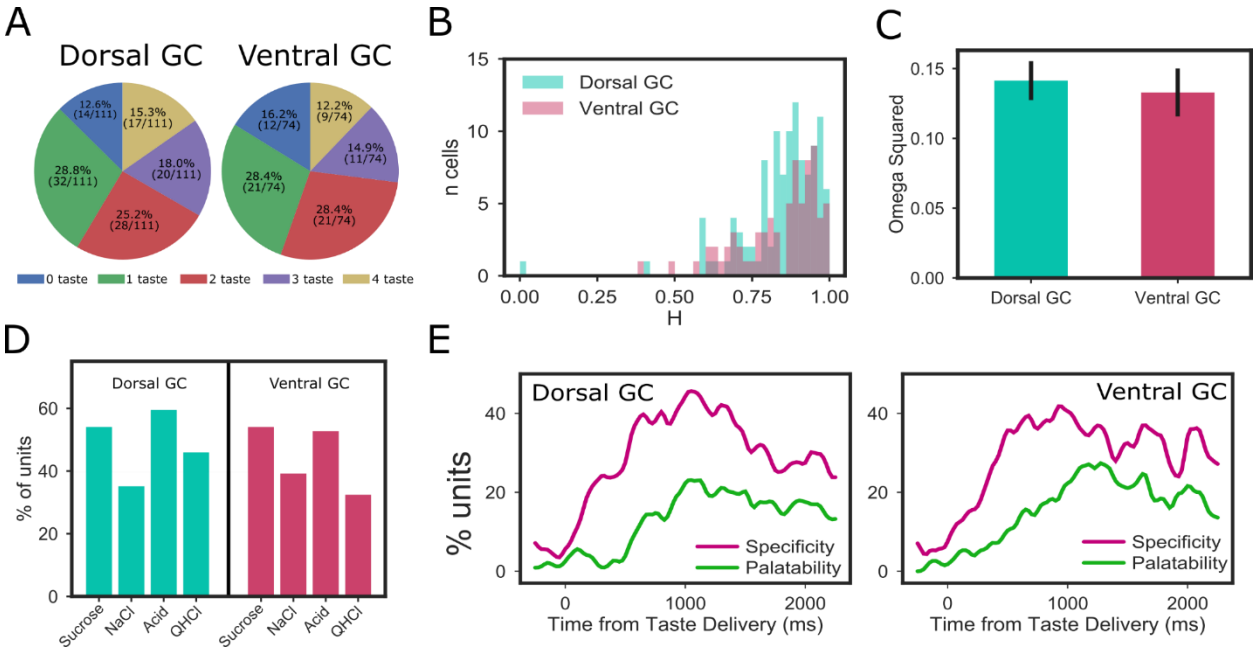

Figure 8. Dorsal and ventral GC taste responses in mice have similar properties. **A**. Percentages of dorsal and ventral neurons with significant responses to zero, one, two, three, and four tastes. X^2 tests revealed no significant differences between the distributions. **B**. Response entropies (H) for dorsal and ventral GC neurons were not significantly different, according to X^2 tests comparing the distributions. **C**. The magnitudes of taste specificity (expressed as omega squared from 2-way ANOVAs, see Methods for details) for dorsal and ventral GC neurons. T-test revealed no difference. **D**. The distribution of relative responsiveness to the four tastes is virtually identical in dorsal and ventral GC—a X^2 test did not suggest any differences in which subregion responded to which tastes. **E1-2**. In both dorsal and ventral GC, taste specificity starts to rise immediately after taste delivery and peaks at 500ms, and in both, the emergence and peaking of palatability-related firing was delayed (see Figure 5).

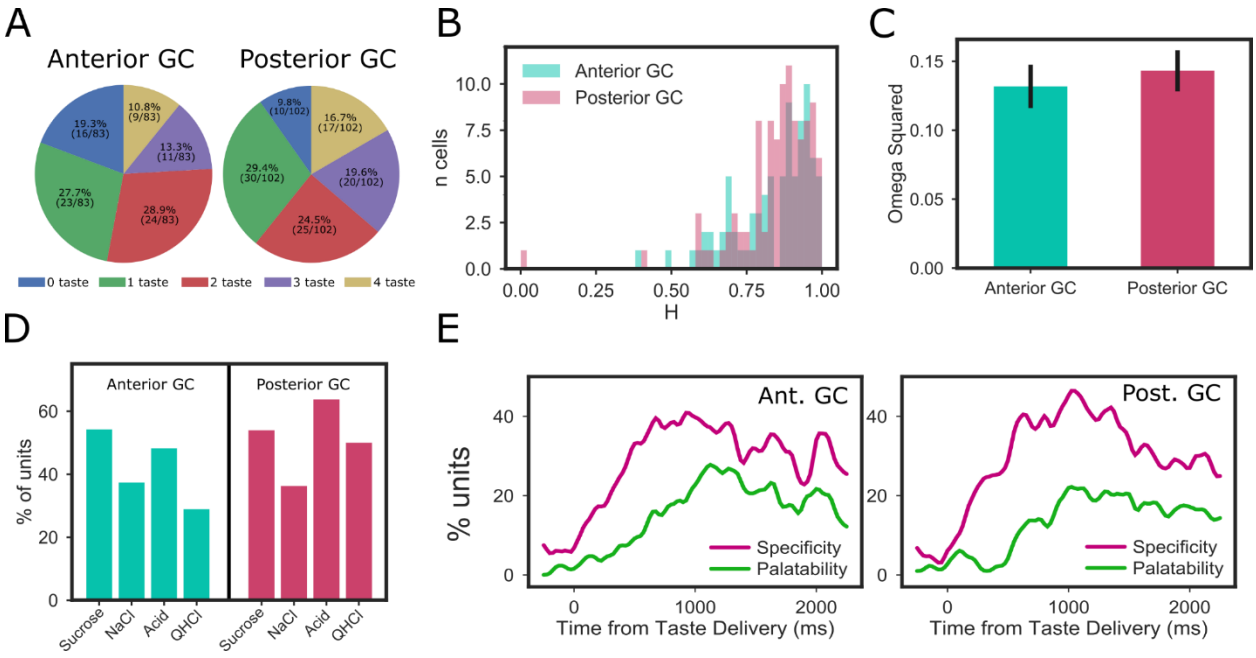

Figure 9. Anterior and posterior GC taste responses in mice have similar properties. **A**. Percentages of anterior and posterior neurons with significant responses to zero, one, two, three, and four tastes. X^2 tests revealed no significant differences between the distributions. **B**. Response entropies (H) for anterior and posterior GC neurons were not significantly different, according to X^2 tests comparing the distributions. **C**. The magnitudes of taste specificity (expressed as omega squared from 2-way ANOVAs, see Methods for details) for anterior and posterior GC neurons. T-test revealed no difference. **D**. The distribution of relative responsiveness to the four tastes in posterior GC was similar to that in anterior GC; while responsiveness to the two more aversive tastes was somewhat higher in posterior GC, a X^2 test did not reveal any significant differences in which subregion responded to which tastes. **E1-2**. In both anterior and posterior GC, taste specificity starts to rise immediately after taste delivery and peaks at 500ms, and in both, the emergence and peaking of palatability-related firing was delayed (see Figure 5).